



## Phylogeny, genetic variability and colour polymorphism of an emerging animal model: The short-lived annual *Nothobranchius* fishes from southern Mozambique

A. Dorn<sup>a,1</sup>, E. Ng'oma<sup>a,1</sup>, K. Janko<sup>b,1</sup>, K. Reichwald<sup>a,1</sup>, M. Polačik<sup>c</sup>, M. Platzer<sup>a</sup>, A. Cellerino<sup>a,d,\*\*</sup>, M. Reichard<sup>c,\*</sup>

<sup>a</sup> Leibniz Institute for Age Research – Fritz Lipmann Institute, Beutenbergstrasse 11, 07745 Jena, Germany

<sup>b</sup> Institute of Animal Physiology and Genetics, Academy of Sciences of the Czech Republic, Rumburská 89, 277 21 Liběchov, Czech Republic

<sup>c</sup> Institute of Vertebrate Biology, Academy of Sciences of the Czech Republic, Květná 8, 603 65 Brno, Czech Republic

<sup>d</sup> Scuola Normale Superiore, Piazza dei Cavalieri 7, 56100 Pisa, Italy

### ARTICLE INFO

#### Article history:

Received 12 December 2010

Revised 8 June 2011

Accepted 10 June 2011

Available online 25 June 2011

#### Keywords:

Ageing

Allopatric speciation

Cyprinodontiformes

Killifish

Life history

Mozambique

### ABSTRACT

*Nothobranchius* are a group of small, extremely short-lived killifishes living in temporary savannah pools in Eastern Africa and that survive annual desiccation of their habitat as dormant eggs encased in dry mud. One mitochondrial (*COI*) and three nuclear (*CX32.2*, *GHITM*, *PNP*) loci were used to investigate the phylogenetic relationship of *Nothobranchius* species from southern and central Mozambique. This group shows marked variation in captive lifespan at both the inter- and intraspecific levels; lifespan varies from a few months to over a year. As their distribution encompasses a steep gradient between semi-arid and humid habitats, resulting in contrasting selection pressures on evolution of lifespan and associated life history traits, Mozambican *Nothobranchius* spp. have recently become a model group in studies of ageing, age-related disorders and life history evolution. Consequently, intraspecific genetic variation and male colour morph distribution was also examined in the recovered clades. Using Bayesian species tree reconstruction and single loci analyses, three large clades were apparent and their phylogenetic substructure was revealed at the inter- and intra-specific levels within those clades. The *Nothobranchius furzeri* and *Nothobranchius orthonotus* clades were strongly geographically structured. Further, it was demonstrated that male colour has no phylogenetic signal in *N. furzeri*, where colour morphs are sympatric, but is associated with two reciprocally monophyletic groups in *Nothobranchius rachovii* clade, where colour morphs are parapatric. Finally, our analysis showed that a polymorphism in the *Melanocortin1 receptor* gene (which controls pigmentation in many vertebrates and was a candidate gene of male colouration in *N. furzeri*) is unrelated to colour phenotypes of the study species. Our results raise significant implications for future comparative studies of the species and populations analysed in the present work.

© 2011 Elsevier Inc. All rights reserved.

### 1. Introduction

The genus *Nothobranchius* represents a group of small fishes that inhabit temporary savannah pools in Eastern Africa. The genus currently comprises 57 valid species (Froese and Pauly, 2010), distributed from southern Sudan to KwaZulu Natal in South Africa. Most *Nothobranchius* species are distributed in lowland plains,

though a significant number of species occur at higher altitude on the plains of Kenya, Tanzania and Zimbabwe (Wildekamp, 2004). The pools inhabited by *Nothobranchius* are not parts of river systems, but they may occasionally be flooded during the peak rainy season, either from adjacent streams or through connection with neighbouring pools when large parts of savannah get flooded. All *Nothobranchius* species are annual; the adults die when the habitat dries out and the next generation survives in the form of desiccation-resistant eggs encased in dry mud. The eggs hatch after the onset of the rainy season, develop and grow rapidly, and can reach sexual maturity at only three weeks (Genade et al., 2005; Valdesalici and Cellerino, 2003). At sexual maturity, the fish reproduce daily until the habitat dries out. *Nothobranchius* are genetically determined as short-lived and their captive lifespan is limited from a few months to over 1 year, depending on the species

\* Corresponding author. Fax: +420 543 211 346.

\*\* Co-corresponding author. Contributed equally to project supervision.

E-mail addresses: [adorn@fli-leibniz.de](mailto:adorn@fli-leibniz.de) (A. Dorn), [enoch@fli-leibniz.de](mailto:enoch@fli-leibniz.de) (E. Ng'oma), [janko@iapg.cas.cz](mailto:janko@iapg.cas.cz) (K. Janko), [kathrinr@fli-leibniz.de](mailto:kathrinr@fli-leibniz.de) (K. Reichwald), [polacik@ivb.cz](mailto:polacik@ivb.cz) (M. Polačik), [mplatzer@fli-leibniz.de](mailto:mplatzer@fli-leibniz.de) (M. Platzer), [acellerino@sns.it](mailto:acellerino@sns.it) (A. Cellerino), [reichard@ivb.cz](mailto:reichard@ivb.cz) (M. Reichard).

<sup>1</sup> Co-first authors. These authors contributed equally.

(Genade et al., 2005). Their rapid development, short lifespan, expression of ageing-related markers and age-dependent deterioration of physiological functions have led to using them as a model in ageing research (Genade et al., 2005; Herrera and Jagadeeswaran, 2004). In particular, a species group of Mozambican *Nothobranchius* has proved extremely useful (Terzibasi et al., 2007) due to its extremely short lifespan (Valdesalici and Cellerino, 2003), relatively easy captive breeding (Genade et al., 2005) and access to numerous wild populations (Reichard et al., 2009) that differ in lifespan, expression of age markers and age-related physiological changes (Terzibasi et al., 2008). Importantly, different captive strains of *Nothobranchius furzeri* Jubb, originating from different locations in its distribution range, show large-scale differences in captive lifespan (Terzibasi et al., 2008). As different populations of *N. furzeri* may represent a useful model system for genetic studies on ageing, genome sequencing has started for this species (Reichwald et al., 2009) and genomic regions controlling simple traits, such as tail colour and sex, have been mapped by linkage analysis (Valenzano et al., 2009). In addition, telomere dynamics (Hartmann et al., 2009) and response to dietary restriction (Terzibasi et al., 2009) have been compared for different geographic strains of *N. furzeri*. In this broader context, it is important to test for the existence of geographical sub-structuring in this species and to further describe the phylogenetic relationships of *N. furzeri* with other species of *Nothobranchius* present within its distribution range.

Six species of *Nothobranchius* inhabit southern Mozambique (Wildekamp, 2004). *Nothobranchius orthonotus* (Peters) has a very wide distribution, with records from KwaZulu Natal in the south to just north of the Zambezi River, including a report from southern Malawi (Wildekamp, 2004). *Nothobranchius kuhntae* Ahl has been described from the Beira region on the lower Pungwe River, though it is often synonymised with *N. orthonotus* based on similarity of colour pattern (Wildekamp, 2004). *Nothobranchius furzeri* is a common species in the savannah regions of the Incomati, Limpopo and Chetu River catchments in southern Mozambique (Reichard et al., 2009), with a single locality also known in Zimbabwe, Sazale Pan at Gona Re Zhou National Park close to the Mozambican border (Jubb, 1971). *Nothobranchius kadleci* Reichard, which inhabits regions between the Save and Zambezi Rivers (Reichard, 2010), is morphologically similar to *N. furzeri* but clearly diagnosable by morphology and colouration. Finally, *Nothobranchius rachovii* Ahl has a wide distribution, which is comparable to that of *N. orthonotus*. The original range of *N. rachovii* was from the Kruger National Park in South Africa to the Kwa-Kwa River north of the Zambezi delta (Watters et al., 2009; Wildekamp, 2004), though it is now extinct in South Africa (Watters et al., 2009). Recently, southern populations formerly assigned to *N. rachovii* were formally described as *N. pienaarri* Shidlovskiy, Watters, Wildekamp and populations north of the Zambezi River as *N. krysanovi* Shidlovskiy, Watters, Wildekamp; with *N. rachovii* sensu stricto inhabiting only a small area near the city of Beira (Shidlovskiy et al., 2010).

All *Nothobranchius* species are sexually dimorphic, with larger colourful males and smaller drab females. Male colouration is sexually selected (Haas, 1976) and many species occur in two colour morphs that can be allopatric or sympatric (Reichard and Polačik, 2010). Some *N. furzeri* males possess a wide yellow sub-marginal band (yellow morph), while other males have a red caudal fin (red morph). The male colour morphs are often sympatric (Reichard et al., 2009) and possibly controlled by a single major locus with yellow dominant over red (Valenzano et al., 2009). The presence of two colour morphs is also known for *N. orthonotus*, though in this case, the red morph is dominant throughout the species' range and only a few yellow (blue) males have ever been captured (Wildekamp, 2004). Only the red male morph has been reported for *N. kuhntae*. Three colour morphs ('black', 'blue' and 'red') with

allopatric distribution are known for *N. rachovii* species complex (Watters et al., 2009; Wood, 2000), recently described as three separate species (Shidlovskiy et al., 2010). Reproductive isolating barriers between *Nothobranchius* colour morphs range from weak to none (Reichard and Polačik, 2010) and it is unclear as to how this polymorphism has evolved and how it has been maintained.

The *Melanocortin 1 receptor* (*Mc1r*) gene was analysed as a candidate gene controlling colour phenotypes in *Nothobranchius* because it is known to mediate skin and hair pigmentation in many vertebrate species, including humans (Hayward, 2003; Valverde et al., 1995; Widlund and Fisher, 2003). In the Mexican cavefish *Astyanax mexicanus*, *Mc1r* has been shown to play a role in the parallel evolution of depigmentation in independent cave populations (Gross et al., 2009). Further, in a recent mapping study of loci associated with yellow/red tail colour in the colour morphs of *N. furzeri*, Valenzano et al. (2009) analysed *Mc1r* of two *N. furzeri* populations (GRZ and MZM-04/03). The study identified a polymorphism in the coding region (G67C), resulting in a change from histidine in GRZ to aspartic acid in MZM-04/03 at amino acid 23 (H23D) in the N-terminal domain of the *Mc1r* protein (Valenzano et al., 2009).

In the present study we investigate the phylogenetic relationships among *Nothobranchius* species from southern Mozambique by the analysis of sequence variations in one mitochondrial (*COI*) and three nuclear (*CX32.2*, *GHITM*, *PNP*) loci in samples covering the majority of the species' ranges. We further test whether *N. furzeri* populations are structured geographically with respect to male colour morphs and whether male colouration has a phylogenetic signal. Finally, the association of the H23 N polymorphism in *Mc1r* is analysed with respect to male colouration in wild populations.

## 2. Material and methods

### 2.1. Sampling

Eighty-four specimens of *N. furzeri*, *N. kadleci*, *N. kuhntae*, *N. orthonotus*, *N. pienaarri* and *N. rachovii* were obtained from 59 localities in southern and central Mozambique (Table 1, Fig. 1). *Fundulosoma thierryi*, a sister taxon to *Nothobranchius* (Murphy and Collier, 1997), was chosen as an outgroup, while *Fundulopanchax gardneri* (a distantly related nothobranchiid) was chosen as an additional outgroup for mitochondrial locus analysis. Most samples were collected in 2008 (code MZCS; 71 specimens; Table 1). Fish were captured by dip net or seine net, identified on the bank and tissue samples (small part of fin) taken. A subsample of the fish caught were preserved in a 5% solution of formaldehyde or 80% ethanol, the remainder being released. For each population, the proportion of males in each colour morph was calculated. Additional samples were obtained from field collections between 2004 and 2007 (codes MOZ, MT, MZM, MZZW; 11 specimens; Table 1) and from established captive populations of known origin (codes GH and GRZ; two specimens; Table 1). If fish were not collected in the wild, a single specimen was taken from each population.

### 2.2. Sample processing

#### 2.2.1. DNA extraction

Each fin clip was incubated overnight in 600  $\mu$ l of digestion buffer (10 mM Tris pH 8.0, 100 mM NaCl, 10 mM EDTA, 0.5% SDS) in the presence of 20  $\mu$ l Proteinase K at 55 °C. A further 600  $\mu$ l of 1:1 phenol–chloroform was added and centrifuged at 12,100 rpm for 10 min. The clear aqueous phase was transferred to a new tube containing 1 ml 100% ethanol, centrifuged at 12,100 rpm for 10 min and decanted. The pellet was washed with 500  $\mu$ l of 70% ethanol and precipitated at 12,100 rpm for 5 min followed by

**Table 1**

List of samples used in the present study. The lab codes used in Figure 2, species identity, population collection code and its river drainage assignment, phenotypic colour, primers used for COI analysis, geographic position of collection point and Genbank accession numbers for respective genes. Samples from type localities are highlighted by an asterisk.

AG-Code	species	Collection code	Drainage	colour	primers COI	GPS location	COI	GHTIM	Cx32.2	PNP
AG239	<i>F. gardneri</i>	aquarium strain	Akure		22 & 23	not available	JN021666			
AG151	<i>F. thierryi</i>	GH 06–5	Ada		132 & 136	S09 41 W00 58	JN021562	JN628456	JN628452	JN628460
AG029	<i>N. furzeri</i>	MZCS 08–09	Limpopo	red	22 & 23	S23 41.6 E32 36.6	JN021572	JN585246	JN585194	JN585201
AG059	<i>N. furzeri</i>	MZCS 08–09	Limpopo	red	22 & 23	S23 41.6 E32 36.6	JN021570			
AG053	<i>N. furzeri</i>	MZCS 08–43	Limpopo	red	22 & 23	S23 18.4 E32 32.1	JN021593			
AG054	<i>N. furzeri</i>	MZCS 08–45	Limpopo	red	22 & 23	S23 27.5 E32 33.9	JN021596	JN585263	JN585177	JN585215
AG062	<i>N. furzeri</i>	MZCS 08–45	Limpopo	red	22 & 23	S23 27.5 E32 33.9	JN021595			
AG040	<i>N. furzeri</i>	MZCS 08–46	Limpopo	red	22 & 23	S23 41.6 E32 36.6	JN021597			
AG018	<i>N. furzeri</i>	MZCS 08–47	Limpopo	red	19 & 21	S24 03.8 E32 43.9	JN021599			
AG055	<i>N. furzeri</i>	MZCS 08–47	Limpopo	red	22 & 23	S24 03.8 E32 43.9	JN021598	JN585264	JN585176	JN585216
AG019	<i>N. furzeri</i>	MZCS 08–50	Limpopo	red	19 & 21	S24 12.9 E32 50.0	JN021600			
AG041	<i>N. furzeri</i>	MZCS 08–50	Limpopo	red	22 & 23	S24 12.9 E32 50.1	JN088722	JN585254	JN585186	JN585209
AG056	<i>N. furzeri</i>	MZCS 08–53	Limpopo	red	22 & 23	S24 22.1 E32 57.0	JN021602	JN585265	JN585175	JN585217
AG021	<i>N. furzeri</i>	MZCS 08–54	Limpopo	red	22 & 23	S24 22.2 E32 57.0	JN021603	JN585243	JN585195	JN585200
AG042	<i>N. furzeri</i>	MZCS 08–54	Limpopo	red	22 & 23	S24 22.2 E32 57.1	JN021601	JN585255	JN585185	JN585241
AG022	<i>N. furzeri</i>	MZCS 08–55	Limpopo	red	19 & 21	S24 21.8 E32 57.7	JN021664			
AG034	<i>N. furzeri</i>	MZCS 08–61	Limpopo	red	22 & 23	S24 14.4 E33 09.8	JN021604	JN585250	JN585190	JN585205
AG063	<i>N. furzeri</i>	MZCS 08–61	Limpopo	red	22 & 23	S24 14.4 E33 09.9	JN021606	JN585270	JN585170	JN585222
AG023	<i>N. furzeri</i>	MZCS 08–121	Limpopo	red	19 & 21	S24 21.5 E32 58.5	JN021584			
AG037	<i>N. furzeri</i>	MZCS 08–121	Limpopo	yellow	22 & 23	S24 21.5 E32 58.5	JN021576	JN585252	JN585188	JN585207
AG136	<i>N. furzeri</i>	MZCS 08–122	Limpopo	red	19 & 21	S24 18.2 E33 02.8	JN021573			
AG141	<i>N. furzeri</i>	MZM 07–03	Limpopo	red	19 & 21	S23 48.5 E32 37.7	JN021614			
AG057	<i>N. furzeri</i>	MZCS 08–119	Incomati	red	22 & 23	S24 25.1 E32 46.7	JN021580	JN585266	JN585174	JN585218
AG036	<i>N. furzeri</i>	MZCS 08–120	Incomati	yellow	22 & 23	S24 19.5 E32 43.2	JN021574	JN585251	JN585189	JN585206
AG046	<i>N. furzeri</i>	MZCS 08–120	Incomati	yellow	22 & 23	S24 19.5 E32 43.2	JN021583	JN585258	JN585182	JN585212
AG058	<i>N. furzeri</i>	MZCS 08–120	Incomati	red	22 & 23	S24 19.5 E32 43.2	JN021581			
AG064	<i>N. furzeri</i>	MZCS 08–120	Incomati	red	22 & 23	S24 19.5 E32 43.2	JN021571			
AG038	<i>N. furzeri</i>	MZCS 08–123	Incomati	yellow	22 & 23	S24 38.8 E32 26.7	JN021575	JN585253	JN585187	JN585208
AG047	<i>N. furzeri</i>	MZCS 08–123	Incomati	yellow	22 & 23	S24 38.8 E32 26.7	JN021663	JN585259	JN585181	JN585242
AG030	<i>N. furzeri</i>	MZCS 08–23	Chefu	yellow	22 & 23	S22 30.5 E32 33.1	JN021585	JN585247	JN585193	JN585202
AG043	<i>N. furzeri</i>	MZCS 08–23	Chefu	yellow	22 & 23	S22 30.5 E32 33.1	JN021578			
AG051	<i>N. furzeri</i>	MZCS 08–23	Chefu	red	22 & 23	S22 30.5 E32 33.1	JN021577	JN585262	JN585178	JN585214
AG060	<i>N. furzeri</i>	MZCS 08–23	Chefu	red	22 & 23	S22 30.5 E32 33.1	JN021582	JN585268	JN585172	JN585220
AG031	<i>N. furzeri</i>	MZCS 08–28	Chefu	red	22 & 23	S22 28.9 E32 37.2	JN021587	JN585248	JN585192	JN585203
AG061	<i>N. furzeri</i>	MZCS 08–28	Chefu	red	22 & 23	S22 28.9 E32 37.2	JN021586			
AG014	<i>N. furzeri</i>	MZCS 08–29	Chefu	red	19 & 21	S22 27.0 E32 38.8	JN021589			
AG052	<i>N. furzeri</i>	MZCS 08–29	Chefu	red	22 & 23	S22 27.0 E32 38.8	JN021588			
AG032	<i>N. furzeri</i>	MZCS 08–33	Chefu	yellow	22 & 23	S22 21.8 E32 41.9	JN021591			
AG044	<i>N. furzeri</i>	MZCS 08–33	Chefu	yellow	22 & 23	S22 21.8 E32 41.9	JN021590	JN585256	JN585184	JN585210
AG033	<i>N. furzeri</i>	MZCS 08–43	Chefu	yellow	22 & 23	S23 18.4 E32 32.1	JN021592	JN585249	JN585191	JN585204
AG045	<i>N. furzeri</i>	MZCS 08–43	Chefu	yellow	22 & 23	S23 18.4 E32 32.1	JN021594	JN585257	JN585183	JN585211
AG140	<i>N. furzeri</i>	MZM 04–10	Chefu	yellow	19 & 21	S22 21.3 E32 43.3	JN021610			
AG152	<i>N. furzeri</i>	MZM 04–14	Chefu	red	19 & 21	S21 35.4 E33 03.1	JN021611			
AG156	<i>N. furzeri</i>	MZM 07–01	Chefu	female	19 & 21	S22 44.3 E32 05.4	JN021612			
AG154	<i>N. furzeri</i>	MZM 07–02	Chefu	female	19 & 21	S22 21.3, E32 43.3	JN021613			
AG142	<i>N. furzeri</i>	MZZW 07–01	Chefu	yellow	19 & 21	S21 48.9 E31 55.9	JN021615			
AG138	* <i>N. furzeri</i>	GRZ	Chefu	yellow	19 & 21	S21 41.0 E31 44.0	JN021566			
AG065	* <i>N. kadleci</i>	MZCS 08–91	Gorongose	red	22 & 23	S20 41.3 E34 06.4	JN021622			
AG082	* <i>N. kadleci</i>	MZCS 08–91	Gorongose	red	19 & 21	S20 41.3 E34 06.4	JN021623			
AG066	<i>N. kadleci</i>	MZCS 08–99	Pungwe	red	22 & 23	S19 17.4 E34 13.8	JN021625	JN585272	JN585168	JN585224
AG083	<i>N. kadleci</i>	MZCS 08–99	Pungwe	red	22 & 23	S19 17.4 E34 13.8	JN021662			
AG067	<i>N. kadleci</i>	MZCS 08–107	Save	red	22 & 23	S21 00.9 E34 27.8	JN021616	JN585273	JN585167	JN585225
AG084	<i>N. kadleci</i>	MZCS 08–107	Save	red	22 & 23	S21 00.9 E34 27.8	JN021618			
AG068	<i>N. kadleci</i>	MZCS 08–108	Save	red	19 & 21	S21 00.7 E34 32.2	JN021619			
AG069	<i>N. kadleci</i>	MZCS 08–112	Save	red	22 & 23	S21 01.8 E34 44.7	JN021620			
AG086	<i>N. kadleci</i>	MZCS 08–112	Save	red	19 & 21	S21 01.8 E34 44.7	JN021621			
AG070	<i>N. orthonotus</i>	MZCS 08–09	Limpopo	red	22 & 23	S23 41.6 E32 36.6	JN021630	JN585275	JN585165	JN585227
AG094	<i>N. orthonotus</i>	MZCS 08–47	Limpopo	red	22 & 23	S24 03.8 E32 43.9	JN021637			
AG072	<i>N. orthonotus</i>	MZCS 08–59	Limpopo	red	19 & 21	S24 17.8 E33 03.4	JN021647			
AG087	<i>N. orthonotus</i>	MZCS 08–67	Limpopo	red	19 & 21	S24 40.4 E33 24.6	JN021645			
AG095	<i>N. orthonotus</i>	MZCS 08–68	Limpopo	red	22 & 23	S24 48.6 E33 30.5	JN021641			
AG091	<i>N. orthonotus</i>	MZCS 08–121	Limpopo	red	22 & 23	S24 21.5 E32 58.5	JN021639	JN585280	JN585160	JN585232
AG093	<i>N. orthonotus</i>	MZCS 08–43	Chefu	red	19 & 21	S23 18.4 E32 32.1	JN021636			
AG071	<i>N. orthonotus</i>	MZCS 08–23	Chefu	red	22 & 23	S22 30.5 E32 33.1	JN021635	JN585276	JN585164	JN585228
AG092	<i>N. orthonotus</i>	MZCS 08–34	Chefu	red	22 & 23	S22 08.8 E32 49.5	JN021640			
AG155	<i>N. orthonotus</i>	MZM 04–16	Chefu	red	19 & 21	S22 01.5 E32 48.0	JN021652			
AG100	<i>N. orthonotus</i>	MZCS 08–120	Incomati	red	22 & 23	S24 19.5 E32 43.2	JN021649			
AG101	<i>N. orthonotus</i>	MZCS 08–124	Incomati	red	22 & 23	S24 35.6 E32 24.3	JN021638			
AG097	<i>N. orthonotus</i>	MZCS 08–99	Pungwe	red	22 & 23	S19 17.4 E34 13.8	JN021642	JN585281	JN585159	JN585233
AG098	<i>N. orthonotus</i>	MZCS 08–105	Save	red	22 & 23	S20 41.1 E34 06.2	JN021631	JN585282	JN585158	JN585234
AG089	<i>N. orthonotus</i>	MZCS 08–108	Save	red	22 & 23	S21 00.7 E34 32.2	JN021632	JN585278	JN585162	JN585230
AG090	<i>N. orthonotus</i>	MZCS 08–112	Save	red	22 & 23	S21 01.8 E34 44.7	JN021633	JN585279	JN585161	JN585231

(continued on next page)

Table 1 (continued)

AG-Code	species	Collection code	Drainage	colour	primers	COI	GPS location	COI	GHTIM	Cx32.2	PNP
AG099	<i>N. orthonotus</i>	MZCS 08–113	Save	red	22 & 23		S21 12.0 E34 43.6	JN021634			
AG096	<i>N. kuhntae</i>	MZCS 08–97	Rio Savane	red	19 & 21		S19 45.8 E34 54.2	JN021628			
AG074	* <i>N. kuhntae</i>	MZCS 08–98	Rio Savane	red	19 & 21		S19 45.1 E34 56.0	JN021629	JN628454	JN628450	JN628458
AG024	<i>N. kuhntae</i>	MOZ 04–07	Zangue	red	19 & 21		not available	JN021624	JN628453	JN628449	JN628457
AG144	<i>N. kuhntae</i>	MT 03–04	Nhangau	red	19 & 21		S19 43 E35 01	JN021627	JN628455	JN628451	JN628459
AG105	<i>N. pienaar</i>	MZCS 08–81	Inharrime	black	19 & 21		S24 13.7 E34 50.4	JN021564	JN585283	JN585157	JN585235
AG135	<i>N. pienaar</i>	MZCS 08–81	Inharrime	black	19 & 21		S24 13.7 E34 50.4	JN021565			
AG113	<i>N. pienaar</i>	MZCS 08–98	Rio Savane	black	19 & 21		S19 45.1 E34 56.0	JN021661	JN585285	JN585155	JN585239
AG115	<i>N. pienaar</i>	MZCS 08–113	Save	black	19 & 21		S21 12.0 E34 43.6	JN021655	JN585286	JN585154	JN585240
AG106	<i>N. rachovii</i>	MZCS 08–94	Pungwe	blue	19 & 21		S19 25.4 E34 20.4	JN021660			
AG134	<i>N. rachovii</i>	MZCS 08–100	Buzi	blue	19 & 21		S19 58.6 E34 09.9	JN021646			
AG108	<i>N. rachovii</i>	MZCS 08–103	Buzi	blue	19 & 21		S19 56.9 E34 18.3	JN021653	JN585287	JN585152	JN585237
AG132	* <i>N. rachovii</i>	MT 03–01	Beira	blue	19 & 21		S19 49 E34 55	JN021648			

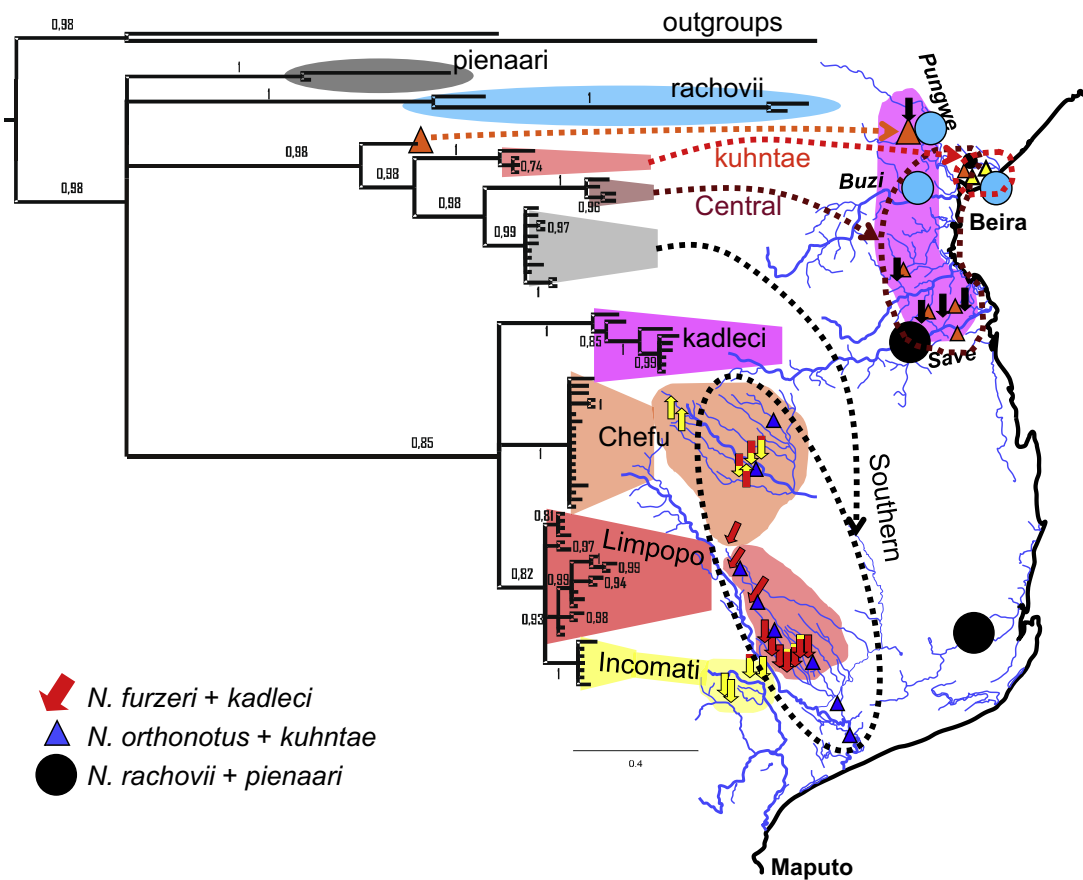


Fig. 1. Map of the study area, with the collection sites of populations mapped onto the hydrographic network of southern and central Mozambique. The COI-based cladogram is colour-coded and linked to the distribution of particular clades. Sampling sites are denoted by species-specific symbols. In *N. furzeri* the proportion of red and yellow colour in the symbol represents the proportion of red and yellow males within the particular population. In all other species, symbol colour denotes inclusion of the sample into the particular geographic clade. Clade distribution is outlined in F-clade. The phylogram of COI sequences is based on Bayesian analysis (MrBayes), with posterior probabilities of the nodes indicated.

decantation and air-drying. The pellet was finally re-suspended in 50  $\mu$ l TE-Buffer (10 mM Tris, 1 mM EDTA, pH 8.0). ([http://kingsley.stanford.edu/Lab%20ProtocolsWEB%20202,003/Fish%20Methods/Stickleback\\_DNA\\_prep.htm](http://kingsley.stanford.edu/Lab%20ProtocolsWEB%20202,003/Fish%20Methods/Stickleback_DNA_prep.htm)).

### 2.2.2. Primer design

Several primers were designed for COI, their position along the COI sequences being shown in Table 2. The first set of primers was designed by aligning the complete sequence of COI from *N. furzeri* (NC\_011814.1) with that of two other Cyprinodontiformes,

*Kryptolebias marmoratus* (NC\_003290.1) and *Cyprinodon rubrofluvialis* (EF442803.2), in order to identify conserved regions. As these primers often failed to amplify COI from species other than *N. furzeri* (*N. rachovii* and *N. pienaar* in particular), a second set of primers was designed by aligning the COI sequences of *N. furzeri*, *N. rachovii*, *N. pienaar* and *F. thierryi* obtained from the previous set of primers in order to obtain *Nothobranchius-versatile* primers. A set of primers for *Mc1r* was prepared based on *N. furzeri* (Genbank accession GQ463613.1). Primers for nuclear loci are listed in Table 2.

**Table 2**  
List of primers used in this study.

Gene	Name	Reference	Position	Primer sequence
<i>COI</i>	22f	NC_011814.1	41–61	AATCAYAAAGATATCGGCAC
<i>COI</i>	20f	NC_011814.1	380–400	ACAGGCTGRACAGTCTATCC
<i>COI</i>	19f	NC_011814.1	537–559	TTTCACARTATCAAACCCC
<i>COI</i>	23r	NC_011814.1	1466–1447	ACWGAAGWACTTCNCGTTT
<i>COI</i>	21r	NC_011814.1	1439–1420	AATGCTTCTCAGAYAATAAA
<i>COI</i>	3r	NC_011814.1	1231–1212	CATGAAGCGTGTAGCTGAA
<i>COI</i>	132f	NC_011814.1	555–577	GACCCAGCTGGWGGAGGAGA
<i>COI</i>	136r	NC_011814.1	1198–1179	CCTGCTAAGCCTAGGAAGTG
<i>GHTM</i>	c11.f1	JN585151	315–334	CGTAAAGAAGGCTGAGACAC
<i>GHTM</i>	c11.r1	JN585151	821–838	CCTCCTCATGCTGATAC
<i>CX32.2</i>	a05.f1	JN585150	537–556	GGGGCAGTATTACCTGTACG
<i>CX32.2</i>	a05.r1	JN585150	1068–1086	GTGACAAACGCTCTGG
<i>PNP</i>	f06.f1	JN585149	370–386	AGCATCCGTTGTGTGGAC
<i>PNP</i>	f06.nf1	JN585149	464–481	AGCTCTGCCCTCATCTTG
<i>PNP</i>	f06.nr1	JN585149	825–842	GAAGGTCTCAGTGTGTGTTG
<i>PNP</i>	f06.r1	JN585149	894–913	GTGACAAACGCTCTGG

### 2.2.3. Pcr

PCRs were performed at 25 µl final volume, each with 2.5 µl 10x PCR buffer; 1.5 µl 25 mM MgCl<sub>2</sub>; 0.5 µl each of 10 mM dNTP mix, 10 µM forward, 10 µM reverse primers, 0.25 µl 5U/µl Taq Polymerase (Qiagen) and 100–150 ng of genomic DNA using an EPPENDORF thermocycler (Mastercycler ep gradients).

The PCR-program for primers 22f–23r and 20f–3r was: 94 °C for 120 s followed by 10 cycles with a touchdown (94 °C for 30 s, touchdown from 55 °C to 50 °C, 0.5 °C decrease at every step) and 30 cycles (94 °C for 30 s, 50 °C for 30 s, 72 °C for 90 s), and a final 180 s at 72 °C. For primers 19f–21r, the same program was used except that touchdown was performed from 51 °C to 46 °C and the annealing temperature was 46 °C. For primers 132f and 136r, the following program was used: 94 °C for 120 s, 35 cycles (94 °C for 30 s, 57 °C for 30 s and 72 °C for 30 s) and 72 °C for 60 s.

PCRs for nuclear loci were as follows: 35 cycles with 30 s at 94 °C, a 30 s at 55 °C and a 1 min at 72 °C. Nested PCRs (1:1000 dilutions of PCR products) were carried out for *PNP*, with 30 cycles of the same cycling profile.

### 2.2.4. Sequencing

Sequencing was performed using the BigDye Terminator v3.1 Cycle Sequencing Kit (ABI; Weiterstadt, Germany), followed by separation on ABI 3730xl capillary sequencers. After quality clipping, sequences were assembled based on overlaps using the GAP4 module of the Staden Sequence Analysis Package as described previously (Reichwald et al., 2009). Visual inspection and manual editing of sequences was undertaken using GAP4.

### 2.3. Phylogenetic reconstructions of individual loci

Phylogenetic analyses were undertaken on two datasets. The first comprised 40 specimens sequenced for all four loci. A second, extended dataset with 81 sequences was used for analysis of *COI*. The *COI* dataset included 34 specimens with suitable sequences for nuclear markers and 47 new specimens. The choice of nuclear loci was based on extensive sequencing of *Nothobranchius* genome. The three nuclear loci (*CX32.2*, *GHTM*, *PNP*) used provided largest polymorphism in pilot sequencing on several individuals. Three markers were chosen as a compromise between reaching sufficient power in analysis and the number of samples (individuals) that can be analysed.

Sequences were aligned using the ClustalW program default settings implemented in the BioEdit software package (Hall, 1999) and then manually checked and edited. For the *COI* dataset, the amino acid translation of the coding sequences was examined for stop codons. The Bayesian method implemented in the Phase 2.0 software (Stephens et al., 2001) was used in an attempt to resolve observed heterozygotes in nuclear loci. The analysis was run at least five times for each locus with different seeds to check for consistency. Despite trying various run conditions and numbers of steps, however, runs were inconsistent and we did not obtain high posteriors for some positions in several specimens. Hence, nuclear sequences were subjected to subsequent phylogenetic analyses with standard one-letter ambiguity symbols.

Phylogenetic analyses were performed on each locus separately using MrBayes v3.1 Bayesian analysis software (Ronquist and Huelsenbeck, 2003). The Bayesian tree for each locus was inferred using models selected by the Akaike information criterion in MrModeltest (<http://www.abc.se/~nylander>). The models were estimated separately for partitions according to the codon position for *COI* locus. The analyses were performed with 10<sup>7</sup> generations sampling every 1000 trees using two parallel runs with four chains. The final burn-in was 40% of the sampled trees; convergences among runs being checked using AWTY software (Wilgenbusch et al., 2004).

### 2.4. Analysis of multilocus data in BEST

The traditional strategy for improving phylogenetic resolution is to increase the number of loci and characters put into a single concatenated data set. This approach, however, may lead to incorrect estimates of species trees (Edwards et al., 2007), especially when the lengths of internal branches are short and ancestral population size large. This is because concatenation assumes the same phylogeny for all loci and no difference between species tree and individual locus trees (Belfiore et al., 2008). Although the confounding effect of stochastic lineage sorting has long been recognised (Takahata, 1989), the incorporation of coalescence methods into multi-species phylogenetics was missing until the recent development of Bayesian Estimation of Species Trees (BEST; Liu, 2008) allowed for stochastic differences of topology of individual locus trees resulting from coalescence in ancestral populations. The resulting species tree is based on the topologies of individual loci. BEST is particularly suitable for data where incongruence in the phylogenetic signal of individual loci is expected, and is claimed to perform better and produce fewer artefactual topologies than the traditional concatenation approach (Edwards et al., 2007).

The datasets of all four loci were analysed using BEST (Liu, 2008) using two parallel runs with four chains for 100 million generations. Independent gamma distributions were used as the prior of  $\theta$ , setting the effective population sizes of uniparentally inherited and haploid mitochondrial DNA loci as one fourth that of autosomal loci (following Liu and Pearl, 2007). The trees thereby obtained were summarised in MrBayes software using the 'sumt' command. In addition, the stability of posterior probabilities for individual clades was analysed during the BEST run, the burn-in always being set to 20 million generations. Two kinds of analysis were performed. In the first, the complete dataset, including all 40 specimens sequenced for all loci, was divided into groups according to morphologically defined species, i.e. one outgroup, *N. rachovii* (including *N. pienaar* which was not recognised at time of analysis as a separate species), *N. orthonotus*, *N. kuhntae*, *N. furzeri* and *N. kadleci*. In the second, *N. furzeri* specimens were further split according to their geographical origin (the Limpopo, Incomati and Chefu drainage basins). This second analysis was undertaken as it has recently been argued that such geographical divisions

have a strong effect on life history traits (Terzibasi et al., 2008). In both analyses, the optimal species tree treating defined groups was defined as 'species'.

### 2.5. Estimation of divergence times

Divergence dates among the main mitochondrial clades were estimated on the second dataset using a Bayesian coalescence approach, as implemented in BEAST 1.5.4 (Drummond et al., 2006; Drummond and Rambaut, 2007). Only the most common haplotype, which was usually basal, was selected for each major mitochondrial clade for this analysis because we were interested in the dating of divergence between major phylogenetic lineages only. Since BEAST only allows a limited number of substitution models, the models were ranked in jModelTest (Posada, 2008) and that with the lowest AIC score selected. The HKY + G + I model, with Jeffreys prior for substitution rates and gamma values of the jModelTest output, was applied with an uncorrelated lognormal relaxed molecular clock (Drummond et al., 2006). A normally distributed prior with a mean of 0.007 and standard deviation of 0.0010 was used for the mean mutation rate. This normal distribution covered the plausible range of 0.70–0.86% substitutions per site per My, as reported in works dealing with mitochondrial fragments in related families of Rivulidae, Cyprinodontidae and Goodeidae (Echelle et al., 2005; Hrbek and Meyer, 2003; Webb et al., 2004), as well as the standard mtDNA molecular clock rate of 2% sequence divergence per Mya. Two types of analysis were run, employing either the Yule or the birth–death process as the tree prior and assuming a constant speciation (extinction) rate per lineage. The search was begun with a UPGMA tree and two independent runs of 30<sup>7</sup> generations were conducted for each analysis. The results were checked for convergence and stationarity of different runs using Tracer 1.4.1 (<http://beast.bio.ed.ac.uk>). After a burn-in of the first 10% of generations, independent runs were

combined using the LogCombiner 1.4.8 module. Finally, the molecular clock tree was summarised using the TreeAnnotator 1.4.8 module, using the medians as node heights.

### 2.6. Evaluation of *N. furzeri* intraspecific differentiation

The partitioning of genetic variance among taxonomic, geographic and colour morphs was measured using Analysis of Molecular Variance (AMOVA; Excoffier et al., 1992), as implemented in ARLEQUIN (Schneider et al., 2008). For the first analysis, we evaluated the significance of partitioning genetic variance between taxonomic groups (*N. furzeri*, *N. kadleci*) and among geographic groups (Limpopo, Chefu, Incomati). In the second, we evaluated the amount of genetic structuration attributable to the distinction of *N. furzeri* into the two colour morphs (red and yellow). As ARLEQUIN does not allow for the correction of genetic distances according to our best-fitting model of DNA substitution, we used the Tamura-Nei distance instead. Significance was always tested using 1000 permutations.

### 2.7. Colour morphs

Two sets of primer pairs covering the coding sequence of *Mc1r* were designed (GeneBank Accession GQ463613). Thirty-two specimens of *N. furzeri*, *N. rachovii*, *N. pienaarri*, *N. kadleci*, *N. kuhntae* and *N. orthonotus* were sequenced (Table 3). Genotypes at position 67 with respect to yellow/red morph phenotype were examined and tested for consistency with previously observed variation in male colouration using (1) wild populations and a larger sample of yellow vs. red *N. furzeri* specimens, and (2) other *Nothobranchius* species with colour morphs. PCR conditions and cycling profile were as for nuclear loci (see above), with annealing at 58 °C for primer pair 122/127 and 59 °C for pair 126/125. Sequencing reactions and sequence curation was as for nuclear loci.

**Table 3**  
Summary of *Mc1r* gene data, showing species identity, polymorphism at position 67, colour phenotype, geographic origin, GPS coordinates of sampling location, and Genbank accession numbers.

AG-Code	Species	Allele at nt67	Colour phenotype	Drainage	GPS	Genbank
AG049	<i>N. furzeri</i>	G/G	Red tail	Limpopo	S24 09.6 E32 48.1	JN088717
AG050	<i>N. furzeri</i>	G/G	Red tail	Limpopo	S23 41.6 E32 36.6	JN088716
AG052	<i>N. furzeri</i>	C/C	Red tail	Chefu	S22 27.0 E32 38.8	JN088715
AG054	<i>N. furzeri</i>	G/G	Red tail	Limpopo	S23 27.5 E32 33.9	JN088714
AG055	<i>N. furzeri</i>	G/G	Red tail	Limpopo	S24 03.8 E32 43.9	JN088713
AG057	<i>N. furzeri</i>	G/G	Red tail	Limpopo	S24 25.1 E32 46.7	JN088712
AG061	<i>N. furzeri</i>	C/C	Red tail	Chefu	S22 28.9 E32 37.2	JN088711
AG177	<i>N. furzeri</i>	C/C	Red tail	Chefu	S22 30.5 E32 33.1	JN088710
AG178	<i>N. furzeri</i>	C/C	Red tail	Chefu	S22 30.5 E32 33.1	JN088709
AG179	<i>N. furzeri</i>	C/C	Red tail	Chefu	S23 06.0 E32 21.7	JN088708
AG182	<i>N. furzeri</i>	C/C	Yellow tail	Chefu	S23 41.6 E32 36.6	JN088707
AG186	<i>N. furzeri</i>	C/C	Red tail	Chefu	S22 30.5 E32 33.1	JN088718
AG188	<i>N. furzeri</i>	C/C	Yellow tail	Chefu	S22 30.5 E32 33.1	JN088706
AG065	<i>N. kadleci</i>	C/C	Red body + tail	Save	S20 41.3 E34 06.4	JN088694
AG066	<i>N. kadleci</i>	C/C	Red body + tail	Save	S19 17.4 E34 13.8	JN088721
AG067	<i>N. kadleci</i>	C/C	Red body + tail	Save	S21 00.9 E34 27.8	JN088693
AG068	<i>N. kadleci</i>	C/C	Red body + tail	Save	S21 00.7 E34 32.2	JN088692
AG069	<i>N. kadleci</i>	C/C	Red body + tail	Save	S21 01.8 E34 44.7	JN088691
AG081	<i>N. kuhntae</i>	G/G	Red	Beira	Not available	JN088705
AG101	<i>N. orthonotus</i>	C/C	Red	Incomati	S24 35.6 E32 24.3	JN088704
AG104	<i>N. pienaarri</i>	G/G	Melanistic	Limpopo	S24 40.4 E33 24.6	JN088703
AG105	<i>N. pienaarri</i>	G/G	Melanistic	Limpopo	S24 13.7 E34 50.4	JN088702
AG107	<i>N. rachovii</i>	G/G	Orange	Buzi	S19 58.6 E34 09.9	JN088719
AG108	<i>N. rachovii</i>	G/G	Orange	Buzi	S19 56.9 E34 18.3	JN088720
AG110	<i>N. pienaarri</i>	G/G	Melanistic	Limpopo	S23 18.4 E32 32.1	JN088701
AG111	<i>N. pienaarri</i>	G/G	Melanistic	Limpopo	S24 48.6 E33 30.5	JN088700
AG113	<i>N. pienaarri</i>	G/G	Melanistic	Limpopo	S19 45.1 E34 56.0	JN088699
AG116	<i>N. pienaarri</i>	G/G	Melanistic	Limpopo	S24 25.1 E32 46.7	JN088698
AG133	<i>N. pienaarri</i>	G/G	Melanistic	Limpopo	Not available	JN088697
AG162	<i>N. rachovii</i>	G/G	Orange	Beira	S19 49 E34 55	JN088696
AG170	<i>N. rachovii</i>	G/G	Orange	Beira	S19 48.8 E34 54.3	JN088695
AG143	<i>N. pienaarri</i>	G/G	Melanistic	Limpopo	S24 17.7 E32 33.8	JN088690

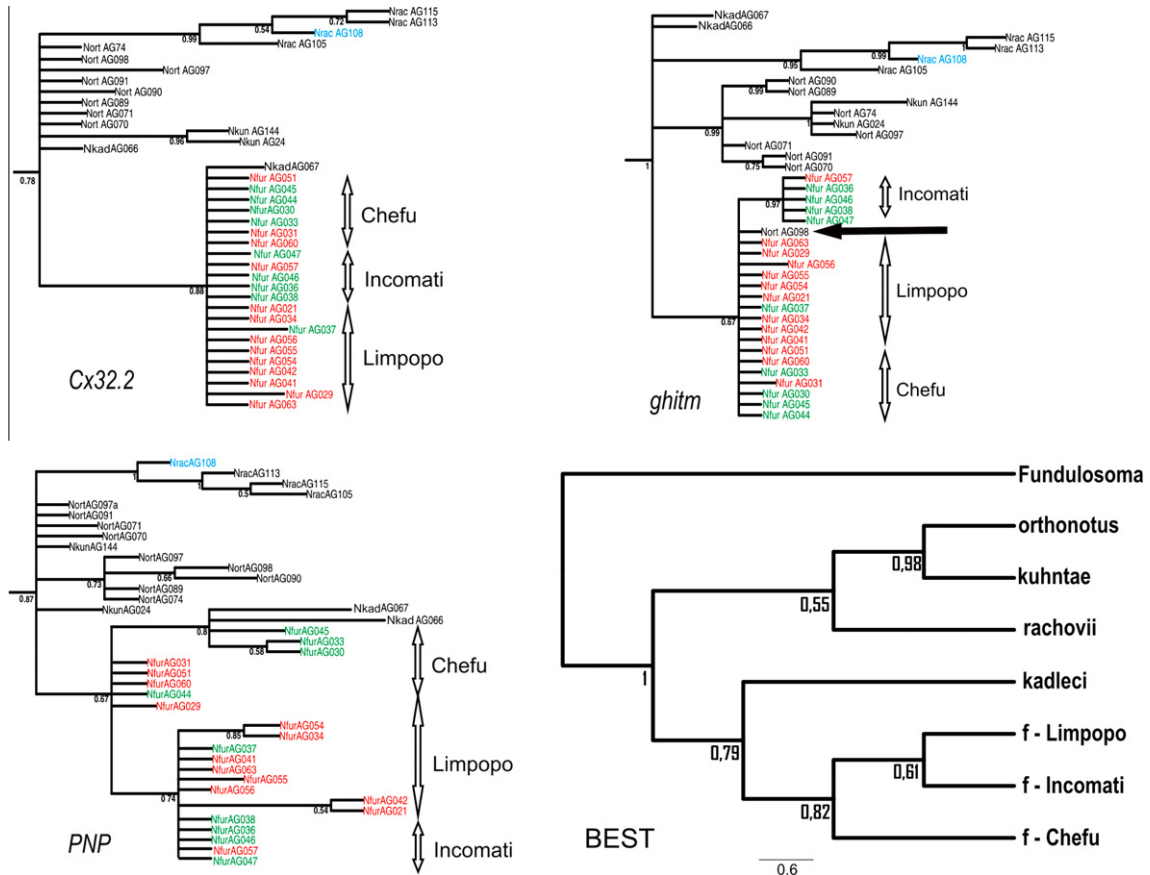


**Fig. 2.** Phylogenetic relationships among *Nothobranchius* specimens reconstructed by MrBayes, using gene trees for *CX32.2*, *ghitm* and *PNP*; and the species tree obtained using the BEST approach. Bayesian posterior probabilities (only BPP > 0.50) for nodal support are shown. In each gene tree, the morphs of *N. furzeri* are indicated by red (red morph) and green (yellow morph) text and *N. rachovii* sensu stricto by blue text. The geographical origin of *N. furzeri* specimens is indicated with vertical lines. The black arrow in the *GHITM* gene phylogram indicates a *N. orthonotus* specimen that clustered with *N. furzeri*. The BEST species tree was based on 40 specimens sequenced for all loci; with *N. furzeri* specimens being split according to their geographical origin (Limpopo, Incomati and Chefu) in order to test the robustness of drainage divisions (see Methods for more details).

Phenotypic data for *N. furzeri* colour morphs was collected in the field in 2008. At least five males were collected from 15 independent populations for inclusion in phenotypic analysis (mean 33 males, range 5–111 males per population). ANOVA was used to test the relative proportion of colour morphs among the three *N. furzeri* clades (Incomati, Chefu, Limpopo). Data were square root arcsin transformed prior to analysis to restore normality of proportional data.

### 3. Results

#### 3.1. Phylogeny of *Nothobranchius* spp. from southern Mozambique

Single nuclear loci often did not resolve phylogeny with high posterior probabilities, presumably due to the low sequence variability (Fig. 2, Table 4). However, nuclear loci consistently suggested monophyly of *N. rachovii* + *N. pienaar* (hereafter referred to as the R-clade). Occasionally, the nuclear loci suggested monophyly of sequences derived from the remaining species/clades with reasonably high posteriors (*N. kuhntae* or *N. orthonotus/kuhntae* clade in *CX32.2* and *GHITM*, respectively, and monophyly of *N. furzeri* sequences from the Incomati watershed in *GHITM*). A notable exception was a single *N. orthonotus* specimen (AG098), which clustered with *N. furzeri* in *GHITM*.

The mitochondrial *COI* locus provided much better support for monophyly within the various species (and even for intraspecific differentiation, see below) but the posterior probabilities for de-

**Table 4**

Summary of sequence variability observed at four studied loci, showing length of sequences (Length), number of variable position (Var), number of parsimony informative sites (Inform), mean pairwise differences ( $\pi$ ) and substitution model (Model). The last two columns are based only on ingroup sequences.

Locus	Length	Var	Inform	$\pi \pm$ s.d.	Model
COI	665	156		0.0174 ± 0.0035	
	1st position	32	15		GTR + I + G
	2nd position	4	0		F81
	3rd position	187	153		GTR + G
GHTIM	570	48	26	0.0067 ± 0.0015	HKY + G
CX32.2	453	37	9	0.0018 ± 0.0014	JC
PNP	536	34	13	0.0064 ± 0.0018	TrN + I

per nodes were also rather low (Fig. 1). There was high support for monophyly of the *N. orthonotus/kuhntae* clade (0.98; henceforth referred to as the O-clade), with *N. orthonotus* and *N. kuhntae* being placed into separate clusters, though a single *N. orthonotus* specimen from the central Pungwe region appeared as basal to both clusters. *Nothobranchius orthonotus* *COI* sequences, therefore, were paraphyletic to *N. kuhntae*. In addition, *N. orthonotus* appears to be structured into a southern (south of the Save river) and central (north of the Save river) clade (Fig. 1). Monophyly of the *N. furzeri/kadleci* clade (henceforth termed the F-clade) was also indicated, with a posterior of 0.85. This clade was strongly differentiated into four main lineages, corresponding to *N. kadleci*, *N. furzeri* from the Chefu drainage, *N. furzeri* from the Incomati drainage and *N. furzeri*

**Table 5**

Results of Bayesian coalescent-based estimation of divergence dates and time to the most recent common ancestor (tMRCA) of selected haplotypes from different populations/species. Median values are given with 95% highest posterior density in parentheses.

Species/population	Divergence time or t <sub>MRCA</sub> in Mya
<i>N. furzeri</i> Incomati vs. Limpopo	0.875 (0.034–3.63)
O-clade	3.32 (0.47–8.67)
F-clade	4.03 (1.07–9.98)
<i>Nothobranchius</i> (including O-, F- and R-clades)	19.6 (8.53–36.62)

from the Limpopo drainage. Phylogenetic relationships among these clusters, however, are unresolved. Deep differentiation at *COI* was also noted for R-clade. Unlike that for nuclear loci, however, R-clade was clustered in two reciprocally monophyletic clades (corresponding to recent description of *N. pienaarri* as a separate species), with an unresolved relationship to the remaining lineages. *Nothobranchius rachovii* and *N. pienaarri* are geographically parapatric and differentiated by dominant colour of the male body (blue or black, respectively).

BEST suggested monophyly of the O-clade (with high posterior probability) and the F-clade, in agreement with single-locus analyses. Interestingly, unlike tests on individual loci, BEST suggested respective monophyly of *N. furzeri* geographical groups and *N. kadleci*, albeit with relatively poor posterior probability (0.82). BEST analysis was not able to infer the position of the R-clade.

Bayesian coalescent-based estimation of divergence dates and the time to most recent common ancestor (MRCA) of selected haplotypes from different populations/species are shown in Table 5. While confidence intervals are large, it appears that the MRCAs of both the O- and F-clades lived in the Pliocene (median estimates 3.3–4 Mya), while the MRCAs of the Limpopo and Incomati clades date to the Pleistocene (0.9 Mya). Based on our dataset, the MRCA of all *Nothobranchius* species originated in the Miocene (median estimate 20 Mya, range 9–37 Mya).

### 3.2. Differentiation of the F-clade

Hierarchical AMOVA of the F-clade indicated that the among-species component of variation referring to grouping of sequences into *N. kadleci* and *N. furzeri* taxa explained approximately 32% of the total variance ( $F_{CT} = 0.32$ ), though this result was not significant. The splitting of *N. furzeri* sequences according to the three river drainages (Limpopo, Chefu, Incomati groups) explained an additional 58% of variance ( $F_{SC} = 0.58$ ;  $P < 0.05$ ).

*Nothobranchius furzeri* from the Limpopo drainage possessed the highest genetic variability among the three geographical groups studied. Nucleotide diversity was four times higher than in the Incomati clade, and almost three times higher than in the Chefu clade (Table 6). Our data do not allow to further hypothesise on whether the observed differences in genetic variability reflect

demographic history. It is notable, however, that while the Limpopo group did not deviate from neutrality in Tajima's D and Fu's Fs indices, the Chefu group significantly deviated from neutrality (Table 6) and expressed an overrepresentation of rare haplotypes and mutations in terminal branches, characteristic of recently expanded populations.

### 3.3. Colour morphs of *N. furzeri*

The yellow/red colour morphs of *N. furzeri* were not monophyletic. In fact, red and yellow males were intertwined in all phylogenies (Fig. 2). AMOVA, however, detected a significant contribution of male colouration to the overall variance ( $F_{ST} = 0.13$ ). Phenotypic data showed that the three geographic clades differed in the proportion of red and yellow morphs (ANOVA,  $F_{2,12} = 30.6$ ,  $P < 0.001$ ), with red males clearly dominating in the Limpopo clade (96 % red), yellow males dominating the Incomati clade (95 % yellow) and a combination of both morphs in the Chefu clade (54 % red, 46% yellow). The AMOVA result therefore, could stem from covariation of colour and geographic origin. *Nothobranchius kadleci* differed markedly from *N. furzeri* colouration and distinct colour phenotypes could not be detected.

### 3.4. Analysis of the *Mc1r* gene

The +67 G > C sequence variation in the *Mc1r* gene was not associated with male colouration. In *N. furzeri*, GG genotypes were found in all five red males from the Limpopo clade, but CC genotypes were present in all Chefu clade fish, including six red and two yellow males (Table 3). In *N. kadleci*, which is characterised by an entirely red colouration, the CC genotype was found in all five specimens analysed. In contrast, the GG genotype was found in *N. kuhntae* (red colouration, one individual), *N. rachovii* (with a significant red colour component; four individuals) and *N. pienaarri* (a melanistic form with less red colour component; eight individuals).

## 4. Discussion

### 4.1. Inter-specific relationships and structure of the O- and R-clades

Our analyses indicate that Mozambican *Nothobranchius* are deeply structured into several evolutionary lineages. The analyses of one mitochondrial locus (*COI*) and the combined dataset of one mitochondrial and three nuclear loci (BEST) indicate the existence of an F-clade composed of two morphologically distinct species, *N. furzeri* and *N. kadleci*, that are further geographically substructured. The separate analyses of *COI* and *GHITM* loci and BEST analyses support the existence of a lineage composed of *N. orthonotus* and *N. kuhntae* (O-clade). The third lineage (R-clade) was consistently monophyletic in all individual nuclear loci analyses, though the mitochondrial locus did not resolve monophyly.

**Table 6**

Summary of *COI* gene sequence variability in the four F-clade populations examined, with haplotype diversity (*h*), nucleotide diversity ( $\pi$ ) and estimates of Tajima's D and Fu's Fs shown. Significant deviations from neutrality are indicated by asterisks.

Species-population	<i>h</i> ± s.d.	$\pi$ ± s.d.	Tajima's D	Fu's Fs
<i>N. kadleci</i>	0.9333 ± 0.0773	0.008823 ± 0.005243	−1.58144*	−2.02504
<i>N. furzeri</i> -Limpopo	0.9263 ± 0.0316	0.005995 ± 0.003598	−0.36677	−2.69938
<i>N. furzeri</i> -Incomati	0.4643 ± 0.2000	0.001434 ± 0.001320	−1.44751	−0.30459
<i>N. furzeri</i> -Chefu	0.6082 ± 0.1272	0.002129 ± 0.001522	−2.05915**	−2.59351*

\*  $P < 0.05$ .\*\*  $P < 0.01$ .

All three clades have a wide distribution within the sampled area (Reichard et al., 2009). The F-clade is more common at higher altitudes further away from the Indian Ocean, and never found in coastal areas. The R-clade is frequently found on coastal lowland plains as close as 1 km to the Indian Ocean (e.g. the city of Beira), though fish never occur in brackish water (Wildekamp, 2004). Some populations of the R-clade, however, are known from relatively high altitudes, where they live sympatrically with *N. furzeri* (Polačik et al., 2011; Watters et al., 2009), but their occurrence in that region is relatively rare (Reichard et al., 2009). The O-clade has the widest distribution and its geographical and altitudinal range includes the distribution of both F- and R-clades (Wildekamp, 2004), though it is typically the rarest of the syntopic *Nothobranchius* species (Polačik and Reichard, 2010). No other *Nothobranchius* taxa occur in the biogeographical area studied. Geographically closest species to the species included in the present study are *N. kryanovi* from area north of the Zambezi River, *Nothobranchius hengstleri* Valdesalici and *Nothobranchius krammeri* Valdesalici and Hengstler from northern Mozambique, and *Nothobranchius* sp. aff. *kirki* from southern Malawi (Shidlovskiy et al., 2010; Valdesalici, 2007; Valdesalici and Hengstler, 2008; Wildekamp, 2004). While *N. kryanovi* range partially overlaps the range of *N. orthonotus*, the other three species have ranges separated from central and southern Mozambique by the Rift Valley (Pekkala et al., 2008), making their distribution entirely allopatric to all taxa included in this study.

Within the O-clade, *COI* analysis positioned *N. orthonotus* from the River Pungwe drainage (the northernmost *N. orthonotus* population on Fig. 1) at the base of the clade topography, with *N. kuhntae* forming a distinct clade but with no resolution in relation to *N. orthonotus*. Other distinct clades were formed by fish from four populations in the Rio Save and Rio Gorongose drainages (Central clade), and 12 populations from the Limpopo, Chefu and Incomati drainages (Southern clade) (Fig. 1). The fact that a single *N. orthonotus* specimen clustered with *N. furzeri* in *GHITM* analysis indicates a possibility of introgression between the two species; *N. orthonotus* and *N. furzeri* produce viable hybrids in the lab (Polacik and Reichard, 2011) and several specimens morphologically intermediate between the two species were collected in the wild (M. Reichard & M. Polačik, unpublished data).

Within the R-clade, *COI* analysis distinguished two reciprocally monophyletic clades that differ in dominant body colour of the male and were described as separate species (Shidlovskiy et al., 2010) in time of a review process for the current study. *Nothobranchius pienaari*, (formerly 'black morph' of *N. rachovii*), distributed from southern Mozambique (and also historically collected at two sites in the Kruger National Park, South Africa) to within close proximity of the city of Beira, is parapatric with *N. rachovii*, the 'blue morph', yet the two species never co-occur (Watters et al., 2009; Shidlovskiy et al., 2010). The third species (*N. kryanovi*), a 'red morph' of R-clade, occurs north of the Zambezi River (Watters et al., 2009), but no specimen of *N. kryanovi* was available for this study.

#### 4.2. F-clade and intra-specific structure of *N. furzeri*

Within the F-clade, two species are distinguished (*N. furzeri*, *N. kadleci*) with allopatric distribution and distinct colouration. *COI* analysis and *BEST* analysis recovered four well-supported clades that suggest respective monophyly of *N. furzeri* and *N. kadleci*, though posterior probability was relatively poor (Fig. 2). The analysis of *COI* alone did not allow exclusion of paraphyly, or even polyphyly, of *N. furzeri* with respect to *N. kadleci*.

*Nothobranchius furzeri* was clearly geographically structured, with three clades being consistent with drainage separation. It must be reiterated, however, that *Nothobranchius* fishes inhabit

savannah pools that, while they may occasionally be flooded by water from streams, typically represent habitats that are not connected to river systems and their floodplains. Hence, our designations to river basins do not imply a direct role of the hydrographic network in fish dispersal. It is not known how *Nothobranchius* fishes disperse, though the role of exceptionally large floods for juvenile and adult fish, and/or dispersal of eggs in mud attached to large herbivores drinking from the savannah pools, appears most plausible. Our data show that the intraspecific structure of *N. furzeri* is constrained by hydrography and, therefore, fish dispersal during savannah flooding is a more likely explanation. Three specimens from a population originally assigned to the Limpopo drainage (MZCS 08–43) consistently clustered with the Chefu clade. A closer inspection of available maps (Garmin, 2008; Google Earth) could not clearly demonstrate whether the site was situated in the Limpopo drainage or not; however, it is geographically close to the Chefu basin and was tentatively included there.

The three geographic clades also showed remarkable differences in their genetic diversity, with the lowland Limpopo clade showing clearly higher genetic diversity than the higher altitude Incomati and Chefu clades. In addition, Tajima's and Fu's statistics for the Chefu clade are suggestive of a recent expansion. The southern African climate was more arid during the majority of the Pleistocene glacial periods (Finch and Hill, 2008) and the distribution of the higher altitude clades, therefore, may have been reduced to small refugia, with subsequent expansion during the Holocene. Further research using more variable genetic markers (e.g. microsatellites) is necessary to reconstruct population genetic structure at a finer scale and our effort is directed to this end.

The deep geographic structuring of *N. furzeri* has broader relevance for the use of this species in ageing research. The strain derived from Gona re Zhou in Zimbabwe (Fig. 1) is remarkable for its extremely short captive lifespan of about 3 months (Valdesalici and Cellerino, 2003), whereas populations from the lower Chefu and Limpopo clade show lifespans of 6–7 months (Terzibaszi et al., 2008, 2009; Hartmann et al., 2009; Graf et al., 2010). A possible approach to understanding the mechanism(s) responsible for these lifespan differences may be to compare cellular and molecular phenotypes of the short-lived and longer-lived strains, e.g. through analysis of telomere dynamics (Hartmann et al., 2009) or response to dietary restriction (Terzibaszi et al., 2009). A more direct approach, however, would be the crossing of short-lived and longer-lived strains (Valenzano et al., 2009) to identify quantitative trait loci controlling differences in lifespan (Kirschner et al., in preparation). The deep genetic structuring shown by our data provides a guide to the design of future studies such that researchers are able to assess whether the planned comparisons and/or cross entails two strains that belong to different clades.

#### 4.3. Colour morphs

The colour phenotypes observed in *N. furzeri* males showed no phylogenetic signal for either of the loci analysed in this study. While the red morph is dominant in the Limpopo drainage, the proportion of the yellow morph increases in a southwesterly and northwesterly direction in the Incomati and Chefu drainages, respectively (Fig. 1). The two colour morphs are not reproductively isolated (Valenzano et al., 2009) and filial segregation indicates a Mendelian single locus mode of inheritance, with the yellow morph dominant over the red morph (Valenzano et al., 2009). The presence of a very low proportion of yellow males in the Limpopo clade, as opposed to the Chefu and Incomati clades, therefore, further supports the genetic structuring of *N. furzeri*. At present, there are no data allowing us to speculate on whether the geographic structure of colour morphs is a product of genetic drift or has an adaptive basis. It should be noted that the yellow morph

also dominates in marginal areas of the range of *N. furzeri* in the Chefu drainage. Quantitative data were not available for the phenotypic analysis; however, exclusively yellow males have also been recorded on the Gona Re Zhou plateau on the border between Mozambique and Zimbabwe (Jubb, 1971). This is the westernmost population and is at the highest altitude recorded for *N. furzeri* (Terzibasi et al., 2008). The exclusive occurrence of yellow morph has also been recorded in the adjacent MZZW 07/01 population (Fig. 1) on the Mozambique/Zimbabwe border (B. Watters, pers. comm.).

The GRZ strain of *N. furzeri* (widely used in ageing studies) consists of direct descendants from the type locality (upper Chefu drainage, Zimbabwe), which is characterised by an exclusive occurrence of yellow males (Jubb, 1971). Valenzano et al. (2009) showed that GRZ fish showed the genotype +67 CC, whereas red morph fish collected from the Limpopo had the genotype GG. The *Mc1r* gene was analysed because it was linked to the colour locus (Valenzano et al., 2009). The variation results in a non-synonymous change from histidine (H23, GRZ) to aspartic acid (D23, Limpopo) in the N-terminal region of the *Mc1r* protein (Valenzano et al., 2009). A direct role of *Mc1r* has been disputed however, by the observation of some F2 progeny from a cross of a GRZ male and an MZM-0403 female that display either colour and have a GC or GG genotype. Our analysis clearly demonstrated that all 32 wild-caught fish, which include all the clades studied, were homozygous for either allele, but this variability was not associated with fish colouration. We note, however, that only two yellow morph male *N. furzeri* were analysed and both possessed CC genotype. Consequently, while red morph of *N. furzeri* may be associated with both GG and CC genotypes, we cannot exclude the possibility that yellow morph of *N. furzeri* is uniquely associated with CC genotype. Nevertheless, our data indicate that the +67 G > C sequence variation in the *Mc1r* gene is not associated with male colour phenotypes of Mozambican *Nothobranchius* at interspecific level. There remains the possibility that *cis*-regulatory variations upstream of the *Mc1r* gene could be involved in colour phenotypes in *Nothobranchius* (Gross et al., 2009; Mundy, 2009). Further efforts to identify the causative locus are ongoing.

#### 4.4. Summary and conclusions

In summary, a combined analysis of one mitochondrial and three nuclear loci provided several important insights into phylogenetic relationships among Mozambican *Nothobranchius*, a group of annual fish widely used in research on ageing and age-related disorders. Support was provided for the existence of three major clades of *Nothobranchius* in southern Mozambique; an F-clade comprising *N. furzeri* and *N. kadleci*, an O-clade comprising *N. orthonotus* and *N. kuhntae*, and an R-clade comprising *N. rachovii* and *N. pienaarri*. The study further revealed phylogenetic substructure at both the inter- and intra-specific level within those clades. The analyses indicated very strong geographical structure within the F- and O-clades. Although the relative position of these three clades remains unresolved, the data provide a basic framework for future comparative analyses of life history evolution within this group. It has been hypothesised that species and populations from drier habitats experience accelerated ageing due to a short life expectancy constrained by habitat desiccation (Terzibasi et al., 2008). The current dataset revealed that there is considerable geographic clustering and that the recovered clades are associated with regions with distinct environmental conditions. This has significant implications for future comparative studies that use the species and populations analysed in the present work. The results further demonstrated that male colour phenotype has no phylogenetic signal in *N. furzeri* where red and yellow colour morphs are sympatric, but is associated with two distinct lineages in R-clade,

where colour morphs are parapatric. Finally, our analysis showed that polymorphism in the *Mc1r* gene is not related to male colouration.

#### Acknowledgments

Financial support for this study was provided by Czech Science Foundation project No. 206/09/0814 (MR, KJ, MP), Academy of Sciences of the Czech Republic Grant IRP IAPG AV0Z 50450515, and Leibniz Graduate School on Ageing and Age-Related Diseases (LGSA). All fieldwork complied with the legal regulations of Mozambique (collection permit 154/II/2009/DARPE and sample export permit 049MP00518-A/09 of the Mozambican Ministry of Fisheries). We thank Kathleen Seitz, Tom Hofmann, Eileen Powalsky and Heike Harzer for expert technical assistance.

Author contributions: Conceived and designed the work: MR, AC, KJ; sample collection: MR, MPo, AC; molecular analysis: AD, EN, KR, MPI; sequence curation and Genbank submission: KR; phylogenetic analysis: KJ; drafted ms: MR, KJ. All authors contributed to manuscript preparation.

#### References

- Belfiore, N.M., Liu, L., Moritz, C., 2008. Multilocus phylogenetics of a rapid radiation in the genus *Thomomys* (Rodentia: Geomyidae). *Syst. Biol.* 57, 294–310.
- Drummond, A.J., Rambaut, A., 2007. BEAST: Bayesian evolutionary analysis by sampling trees. *BMC Evol. Biol.* 7, 214.
- Drummond, A.J., Ho, S.Y.W., Phillips, M.J., Rambaut, A., 2006. Relaxed phylogenetics and dating with confidence. *PLoS Biol.* 4, 699–710.
- Echelle, A.A., Carson, E.W., Echelle, A.F., Van den Busshe, R.A., Dowling, T.E., Meyer, A., 2005. Historical biogeography of the new-world pupfish genus *Cyprinodon* (Teleostei: Cyprinodontidae). *Copeia* 2005, 320–339.
- Edwards, S.V., Liu, L., Pearl, D.K., 2007. High resolution species trees without concatenation. *Proc. Natl. Acad. Sci. USA* 104, 5936–5941.
- Excoffier, L., Smouse, P.E., Quattro, J.M., 1992. Analysis of molecular variance inferred from metric distances among DNA haplotypes: application to human mitochondrial DNA restriction data. *Genetics* 131, 479–491.
- Finch, J.M., Hill, T.R., 2008. A late quaternary pollen sequence from Mfabeni Peatland, South Africa: reconstructing forest history in Maputaland. *Quatern. Res.* 70, 442–450.
- Froese, R., Pauly, D., 2010. FishBase. <[www.fishbase.org](http://www.fishbase.org)>.
- Garmin, 2008. Garmap Africa Series 2008, Topo and Rec. March ed. MapIT (PTY) Ltd..
- Genade, T., Benedetti, M., Terzibasi, E., Roncaglia, P., Valenzano, D.R., Cattaneo, A., Cellerino, A., 2005. Annual fishes of the genus *Nothobranchius* as a model system for aging research. *Ageing Cell* 4, 223–233.
- Graf, M., Cellerino, A., Englert, C., 2010. Gender separation increases somatic growth in females but does not affect lifespan in *Nothobranchius furzeri*. *PLoS One* 5, e11958.
- Gross, J.B., Borowsky, R., Tabin, C.J., 2009. A novel role for *Mc1r* in the parallel evolution of depigmentation in independent populations of the cavefish *Astyanax mexicanus*. *PLoS Genet.* 5, e1000326.
- Hall, T.A., 1999. BioEdit: a user-friendly biological sequence alignment editor and analysis program for Windows 95/98/NT. *Nucleic Acids Symp. Ser.* 41, 95–98.
- Haas, R., 1976. Sexual selection in *Nothobranchius guentheri* (Pisces-Cyprinodontidae). *Evolution* 30, 614–622.
- Hartmann, N., Reichwald, K., Lechel, A., Graf, M., Kirschner, J., Dorn, A., Terzibasi, E., Wellner, J., Platzer, M., Rudolph, K.L., Cellerino, A., Englert, C., 2009. Telomeres shorten while Tert expression increases during ageing of the short-lived fish *Nothobranchius furzeri*. *Mech. Ageing Dev.* 130, 290–296.
- Hayward, N.K., 2003. Genetics of melanoma predisposition. *Oncogene* 22, 3053–3062.
- Herrera, M., Jagadeeswaran, P., 2004. Annual fish as a genetic model for aging. *J. Gerontol. Ser. A Biol. Sci. Med. Sci.* 59, 101–107.
- Hrbek, T., Meyer, A., 2003. Closing the Tethys sea and the phylogeny of Eurasian Killifishes (Cyprinodontiformes: Cyprinodontidae). *J. Evol. Biol.* 16, 17–36.
- Jubb, R.A., 1971. A new *Nothobranchius* (Pisces, Cyprinodontidae) from Southeastern Rhodesia. *JAKA* 8, 12–19.
- Kirschner, J., Weber, d., Neuschl, C., Franke, A., Zielke, L., Powalsky, E., Groth, M., Shagin, D., Petzold, A., Hartmann, N., Englert, C., Brockmann, G.A., Platzer, M., Cellerino, A., Reichwald, K., in preparation. Mapping of quantitative trait loci controlling lifespan in the short-lived fish *Nothobranchius furzeri* – a new vertebrate model for age research. *Ageing Cell*.
- Liu, L., 2008. BEST: Bayesian estimation of species trees under the coalescent model. *Bioinformatics* 24, 2542–2543.
- Liu, L., Pearl, D.K., 2007. Species trees from gene trees: reconstructing Bayesian posterior distributions of a species phylogeny using estimated gene tree distributions. *Syst. Biol.* 56, 504–514.

- Mundy, N.J., 2009. Conservation and convergence of colour genetics: MC1R mutations in brown cavefish. *PLoS Genet.* 5, e1000388.
- Murphy, W.J., Collier, G.E., 1997. A molecular phylogeny for aplocheiloid fishes (Atherinomorpha, Cyprinodontiformes): the role of vicariance and the origins of annualism. *Mol. Biol. Evol.* 14, 790–799.
- Pekkala, Y., Lehto, T., Mäkitie, H., 2008. GTK Consortium Geological Surveys in Mozambique 2002–2007. Geological Survey of Finland, Special Paper 48. Espoo, 321 pp.
- Polačik, M., Reichard, M., 2010. Diet overlap among three sympatric African annual killifish species (*Nothobranchius* spp.) from Mozambique. *J. Fish Biol.* 77, 754–768.
- Polačik, M., Reichard, M., 2011. Asymmetric reproductive isolation between two sympatric annual killifish with extremely short lifespans. *PLoS ONE* 6, e22684.
- Polačik, M., Donner, M.T., Reichard, M., 2011. Age structure of annual *Nothobranchius* fishes in Mozambique: is there a hatching synchrony? *J. Fish Biol.* 78, 796–809.
- Posada, D., 2008. JModelTest: phylogenetic model averaging. *Mol. Biol. Evol.* 25, 1253–1256.
- Reichard, M., 2010. *Nothobranchius kadleci* (Cyprinodontiformes: Nothobranchiidae), a new species of annual killifish from central Mozambique. *Zootaxa* 2332, 49–60.
- Reichard, M., Polačik, M., 2010. Reproductive isolating barriers between colour-differentiated populations of an African annual killifish, *Nothobranchius korthausae* (Cyprinodontiformes). *Biol. J. Linn. Soc.* 100, 62–72.
- Reichard, M., Polačik, M., Sedláček, O., 2009. Distribution, colour polymorphism and habitat use of the African killifish *Nothobranchius furzeri*, the vertebrate with the shortest life span. *J. Fish Biol.* 74, 198–212.
- Reichwald, K., Lauber, C., Nanda, I., Kirschner, J., Hartmann, N., Schories, S., Gausmann, U., Taudién, S., Schilhabel, M.B., Szafranski, K., Glockner, G., Schmid, M., Cellerino, A., Scharl, M., Englert, C., Platzer, M., 2009. High tandem repeat content in the genome of the short-lived annual fish *Nothobranchius furzeri*: a new vertebrate model for aging research. *Genome Biol.* 10, R16.
- Ronquist, F., Huelsenbeck, J.P., 2003. MrBayes 3: Bayesian phylogenetic inference under mixed models. *Bioinformatics* 19, 1572–1574.
- Schneider, S., Roessli, D., Excoffier, L., 2008. Arlequin: A Software for Population Genetics Data Analysis. Ver 2.0. Genetics and Biometry Lab, Dept. of Anthropology, University of Geneva.
- Shidlovskiy, K.M., Watters, B.R., Wildekamp, R.H., 2010. Notes on the annual killifish species *Nothobranchius rachovii* (Cyprinodontiformes; Nothobranchiidae) with the description of two new species. *Zootaxa* 2724, 37–57.
- Stephens, M., Smith, N.J., Donnelly, P., 2001. A new statistical method for haplotype reconstruction from population data. *Am. J. Human Gen.* 68, 978–989.
- Takahata, N., 1989. Gene genealogy in three related populations: consistency probability between gene and population trees. *Genetics* 122, 957–966.
- Terzibasi, E., Valenzano, D.R., Cellerino, A., 2007. The short-lived fish *Nothobranchius furzeri* as a new model system for aging studies. *Exp. Gerontol.* 42, 81–89.
- Terzibasi, E., Valenzano, D.R., Benedetti, M., Roncaglia, P., Cattaneo, A., Domenici, L., Cellerino, A., 2008. Large differences in aging phenotype between strains of the short-lived annual fish *Nothobranchius furzeri*. *PLoS ONE* 3, e3866.
- Terzibasi, E., Lefrançois, C., Domenici, P., Hartmann, N., Graf, M., Cellerino, A., 2009. Effects of dietary restriction on mortality and age-related phenotypes in the short-lived fish *Nothobranchius furzeri*. *Aging Cell* 8, 88–99.
- Valdesalici, S., 2007. A new species of the genus *Nothobranchius* (Cyprinodontiformes: Nothobranchiidae) from the coastal area of northeastern Mozambique. *Zootaxa* 1587, 61–68.
- Valdesalici, S., Cellerino, A., 2003. Extremely short lifespan in the annual fish *Nothobranchius furzeri*. *Proc. Roy. Soc. Lond. B* 270, 189–191.
- Valdesalici, S., Hengstler, H., 2008. *Nothobranchius krammeri* n. sp. (Cyprinodontiformes: Nothobranchiidae): a new annual killifish from the Meronvi River basin, northeastern Mozambique. *Aqua, Int. J. Ichthyol.* 14, 187–194.
- Valenzano, D.R., Kirschner, J., Kamber, R.A., Zhang, E., Weber, D., Cellerino, A., Englert, C., Platzer, M., Reichwald, K., Brunet, A., 2009. Mapping loci associated with tail color and sex determination in the short-lived fish *Nothobranchius furzeri*. *Genetics* 183, 1385–1395.
- Valverde, P., Healy, E., Jackson, I., Rees, J.L., Thody, A.J., 1995. Variants of the melanocyte-stimulating hormone receptor gene are associated with red hair and fair skin in humans. *Nat. Gen.* 11, 328–330.
- Watters, B.R., Wildekamp, R.H., Cooper, B.J., 2009. *Nothobranchius rachovii* Ahl 1926 – a historical review. *JAKA* 42, 37–76.
- Webb, S.A., Graves, J.A., Macias-Garcia, C., Magurran, A.E., Foighil, D.O., Ritchie, M.G., 2004. Molecular phylogeny of the livebearing Goodeidae (Cyprinodontiformes). *Mol. Phyl. Evol.* 30, 527–544.
- Widlund, H.R., Fisher, D.E., 2003. Microphthalmia-associated transcription factor: a critical regulator of pigment cell development and survival. *Oncogene* 22, 3035–3041.
- Wildekamp, R.H., 2004. A World of Killies: Atlas of the Oviparous Cyprinodontiform Fishes of the World, vol. 4. American Killifish Association, Elyria, OH.
- Wilgenbusch, J.C., Warren, D.L., Swofford, D.L., 2004. AWTY: A System for Graphical Exploration of MCMC Convergence in Bayesian Phylogenetic Inference. <<http://ceb.csit.fsu.edu/awty>>.
- Wood, T., 2000. Trip to Mozambique, 1999. *BKA Killi-News* 2000, 105–107.